Journal of the European Ceramic Society 44 (2024) 2560–2570

Contents lists available at ScienceDirect

Journal of the European Ceramic Society

journal homepage: www.elsevier.com/locate/jeurceramsoc

Fe/Mn oxide-based foams via geopolymerization process as novel catalysts for tar removal in biomass gasification

Annalisa Natali Murri *, Elettra Papa, Valentina Medri *, Francesco Miccio, Elena Landi

National Research Council - Institute of Science, Technology and Sustainability for Ceramics (CNR-ISSMC), Via Granarolo, 64, 48018 Faenza, RA, Italy

ARTICLE INFO

Keywords:
Geopolymerization
Catalyst
Foam
Composite, metal oxides

ABSTRACT

Novel ceramic foams loaded with Fe and Fe/Mn oxides were developed via geopolymerization process as catalysts for tar removal in syngas cleaning operations. The foams were realized through polymer scaffold template replica, by impregnating polyurethane or cellulose foams with a metakaolin based geopolymer slurry loaded with 19 wt% powdered Fe_2O_3 and Mn_2O_3 metal oxides. A thermal treatment up to 900 °C was applied to vitrify and partially crystallize into leucite the geopolymer binder. Foams from cellulose showed better structural properties compared to those from polyurethane. Preliminary test in real gasification conditions were carried out on a lab scale double fixed bed reactor. In working conditions, vitrified phases derived from geopolymer binder promoted the formation of mixed phases of (Fe, Mn) oxides and silicates, beneficial for improving the catalytic activity. Furthermore, foams loaded with mixed Fe-Mn oxides were more effective than granules in reducing the produced tar.

1. Introduction

The ever-growing need for energy is a problem that has been affecting our society on a global scale for several years. Especially if we consider the need to find alternative and sustainable energy sources, which could allow us to no longer rely on increasingly precious non-renewable resources [1–4].

Bioenergy from the burning of biomass fuels is considered as one of the most promising routes for green energy production. Indeed, this technology plays a key role in reducing our dependence on fossil fuels, given the wide availability on a global scale of the resources needed to produce biofuels, as well as the relatively carbon neutrality of such technology [1–4].

Current bioenergy technologies include different methods to convert biomass and residues into energy, the main ones being biochemical and thermochemical processes. The latter includes direct combustion, pyrolysis and gasification processes, among which biomass gasification is considered one of the most cost-effective and efficient way to produce green energy from solid biofuels [5–8].

In gasification, biomass is converted into a combustible gas in an oxygen-depleted environment at elevated temperatures (500–1400 °C) consisting of carbon monoxide, carbon dioxide, methane, nitrogen and water vapor. Such gaseous product can be burned directly to produce heat or used as a fuel (syngas), after the removal of tar and other particulates which form as contaminants during the conversion process [6–10].

Tarry compounds, a complex mixture of condensable hydrocarbons, are renowned for their negative effect on downstream equipment, as they can condense and lead to clogging and fouling problems. Therefore, tarry compounds represent one of the main drawbacks related to this technology. Moreover, tar is harmful to the human health and the environment, owing to its potential carcinogenicity, making it clear that finding strategies for its complete removal from the syngas is a need of primary importance [10–12].

Current strategies used to clean up the syngas include mechanical/physical and thermal methods. Physical ones are based on the separation of tar in its condensed form, using filters and scrubbers, but have the drawback of generating special and noxious wastes [10,11,13]. Contrarily, thermal processes can completely remove tar components, but temperatures higher than 1000 °C are needed, therefore requiring excessive amounts of energy to be competitive. Up to date, one of the most effective methods to reduce the concentration of tar in the syngas is its catalytic reforming: the tar hydrocarbons are converted into lower molecular weight compounds and to gaseous products such as H_2 and CO, increasing the yield of syngas [13–17]. Differently from the thermochemical conversion, the catalytic approach doesn't need high

* Corresponding authors.
E-mail addresses: annalisa.natalimurri@issmc.cnr.it (A. Natali Murri), valentina.medri@issmc.cnr.it (V. Medri).

https://doi.org/10.1016/j.jeurceramsoc.2023.12.005
Received 25 September 2023; Received in revised form 28 November 2023; Accepted 1 December 2023
Available online 4 December 2023

energy amounts, as it allows to reduce the reaction temperature. It is therefore configured as a cost-effective method to achieve the cleaning of syngas without needing to physically collect and dispose the produced tar.

The catalyst used in catalytic gas reforming can vary depending on the feedstock and the desired outcome, but it typically includes metals or natural minerals. There are several types of tar cracking catalysts that have been developed and studied, including catalysts based on metals such as nickel, cobalt, and copper, and catalysts based on minerals such as zeolites and clay. Nickel-based catalysts have been largely used, as they have been found to be effective in breaking down tars in syngas production from biomass and able to effectively improve the yield of syngas during the gasification of biomass [18–22]. However, nickel-based catalysts raise concerns about their toxicity, as it is a known human carcinogen, as also about its environmental impact, for potentially leaching from into the surrounding soil and water. To mitigate these risks, more sustainable catalysts have been studied and developed. Zeolite and clay-based catalysts for example have been investigated and demonstrated to have good ability to crack tars in syngas production from biomass [16,23–25]. Zeolites are a class of microporous crystalline aluminosilicates that have a high surface area and a well-defined pore structure. These properties make them highly effective catalysts for a wide range of chemical reactions, including tar cracking. Zeolites have several advantages over nickel catalysts in tar cracking: they are less toxic, have a lower environmental impact, and are more stable at high temperatures. Additionally, zeolites can be customized to optimize their catalytic properties for specific tar cracking reactions [16,23,25]. Also, iron oxide-based and magnesium oxide-based catalysts have been found to be effective in cracking tars, and compared to nickel-based they are abundant, cost-effective, and non-toxic, and can be easily disposed of [16,26,27].

Catalysts produced via geopolymerization are a relatively new area of research for tar cracking in syngas production [28–31]. Geopolymers are inorganic polymers that are synthesized from aluminosilicate minerals, such as kaolinite and fly ash. The geopolymerization is inherently sustainable in term of raw materials and energy demand. These clay-based materials have good mechanical properties coupled with a nanoporous microstructure, which makes them particularly suitable for use as catalysts [29,32,33]. Geopolymers are indeed considered the amorphous counterpart of zeolites since they present an amorphous to semi-crystalline 3D network composed of nano-precipitates separated by nanopores. Consequently, the geopolymeric material is characterized with an intrinsic mesoporosity (2–50 nm) [34]. The geopolymerization process can be also combined with various foaming methods to allow the widening of the pore size range up to and over the macro-porous region, even reaching the millimetric scale [34,35]. Furthermore, thermal treatments can partially or completely crystallize the structure of the geopolymer [36–38], making it stable and suitable for different operating temperatures. For this reason, the use of catalysts produced through geopolymerization presents numerous advantages for tar cracking compared to traditional catalysts, such as high thermal stability, low cost, and low toxicity. Additionally, catalysts prepared via geopolymerization can be easily modified to improve their catalytic properties by incorporating other elements, such as transition metals, enhancing their catalytic activity [29,31,39,40]: the incorporation of iron or manganese can further lead to a more sustainable catalyst design, at the same time reducing the reliance on precious and rare metals [28, 39,41]. Moreover, geopolymer-based catalysts can be tailored to exhibit excellent selectivity towards specific desired products, as their composition and metal loading can be adjusted to optimize performances for different biomass feedstocks, operating conditions, and desired product distributions [29,31]. This flexibility makes catalysts produced via geopolymerization suitable for various tar reforming applications, accommodating the diverse needs of biomass gasification and pyrolysis processes. Furthermore, the possibility of using monolithic foams compared to granulated materials would favor the efficiency of exploitation of the active phase. This is due to the possibility of regulating the multidimensional interconnected porosity of the material by increasing the gas flow. For the same volume occupied in the reactor chamber, this morphology would also allow the weight of the catalysts to be significantly reduced.

With these premises and based on the findings made in a previous work [28], in this work monolithic ceramic foams were prepared by replica technique using geopolymer slurries loaded with Fe and Fe/Mn oxides, in view of their potential use as catalytic materials for tar removal from syngas. Scientific literature is rare regarding the replica method applied to geopolymer slurries since a thermal treatment is needed to remove the organic template. As an example, Kovářík et al. reported replica method using geopolymers as precursor of open-cell ceramic foam [42,43]. In the present work a thermal treatment was applied to partially crystallize the geopolymer binder into leucite, while the newly formed glassy phases are functional to improve catalytic performance during service by promoting further crystallization of mixed oxides and silicates [28,44]. This study mainly explores the production process of foams, providing an insight on their properties in relevant operating conditions. The aim is to confirm the good performances exhibited by mixed metal oxides-loaded composites also in a monolithic form, after tailoring of the pore network combined with sufficient mechanical properties.

2. Materials and methods

2.1. Geopolymer foamed monoliths

A geopolymer slurry was produced according to a previously developed formulation [28,35], by reacting a commercial metakaolin powder (Argical M-1200S, IMERYS, France) with an aqueous potassium disilicate solution obtained by mixing KOH pellets (purity > 99%, Merck, Germany) in distilled water and adding fumed silica powder (99.8% Merck, Germany) under magnetic stirring, up to obtain molar ratios of $SiO_2/K_2O = 2.0$ and $H_2O/K_2O = 13.5$. The geopolymer slurry was mixed using a planetary centrifugal mixer (Thinky Mixer ARE-500, Thinky Corporation, Japan) for 1 min at 900 rpm; metal oxide Fe_2O_3 (325 mesh, 98%<5 μm, MRC) and Mn_2O_3 (325 mesh, 99%< 44 μm, Sigma-Aldrich, Germany) powders with Sauter mean diameter respectively of 2 and 3 μm and 90% of particles with diameter respectively lower than 1.5 and 8.9 μm after sonication [28]. The oxide powders were added in measure of 19.4 wt% on the total mixture, as well as extra water to achieve the proper workability of the slurries. The mixtures were further mixed for another 2 min at 900 rpm. The obtained formulations are resumed in Table 1.

The two geopolymer formulation were then used to impregnate polyurethane and cellulose-based sponge templates with a prismatic (18 ± 1 mm length x 22 ± 1 mm width x 25 ± 1 mm height) and cylindrical (22 ± 1 mm diameter x 25 ± 1 mm height) shape respectively. The scaffolds were obtained by soaking the selected templates in the geopolymer mixtures and removing the excess liquid by squeezing out the foams. The samples obtained from the two formulations were consistently labeled as GFe-P, GFe-C, GMnFe-P, GMnFe-C, where P and C respectively indicate the polyurethane and the cellulose-based scaffold template. The impregnated scaffolds were firstly cured at 80 °C for 24 h, followed by 24 h curing at room temperature, then heat treated at 600 °C for one hour in air (heating ramp at 50 °C/h) to burn out the organic templates and subsequently for further two hours at 900 °C

Table 1
Geopolymer formulations.

Formulation	SiO_2/Al_2O_3 (molar)	K_2O/Al_2O_3 (molar)	Fe_2O_3 [wt%]	Mn_2O_3 [wt%]	L/S wt/wt
GFe	4.0	0.8	19.4	0	0.7
GMnFe	4.0	0.8	9.7	9.7	0.7

(heating ramp at 100 °C/h). The literature reports that the crystallization initiation temperature of the leucite from geopolymers ranges from 800 °C to 1050 °C, also depending on the holding time [36–38]. The process temperature of 900 °C was kept uniform with the operating temperatures (see par. 2.3) and such as not to favor a complete crystallization of the geopolymers.

2.2. Characterization techniques

The geometrical density of the foams was determined by weight-to-volume ratio on samples after the burnout of the organic template material and subsequent thermal treatment up to 900 °C. The total porosity, including both open and closed porosity, was calculated as the ratio between the foam geometrical density and the true density of the material measured with helium pycnometry (2.355 g/cm^3 and 2.346 g/cm^3 respectively for powdered GFe and GMnFe foams).

Mercury intrusion porosimetry (MIP) was used to determine the cumulative open pore volume and pore size distribution of the strut material in the range 0.0058 – 100 μm, as well as specific surface area (Thermofinnigan Pascal 140/240).

Optical microscopy analysis was carried out on the foams to evaluate their macrostructure and the foam cell distribution by means of a digital microscope (HIROX RH-2000, Hirox, Japan). The materials microstructure was investigated by scanning electron microscopy (SEM), using an environmental electron scanning microscope ESEM (Quanta 200, FEI-Thermo Fisher Scientific, USA) and a field emission electron scanning microscope FE-SEM equipped with energy dispersion spectroscopy (EDS) probe (ZEISS SIGMA, Carl Zeiss Microscopy GmbH), to assess the elemental composition and distribution in the materials.

The dimensional distributions of the macro-pores of the foams were obtained by analyzing high-resolution images with the open-access ImageJ software [45]. Feret diameters were used for the macro-pore distributions.

The mineralogical phase composition of the geopolymer materials was determined by X-Ray powder diffractometry (XRD) using a Bruker D8 Advance (Bruker – Karlsruhe, Germany) diffractometer.

Permeability tests were carried out in a laboratory plant (Fig. 1) consisting of an electronic mass-flow meter and controller (Brooks mod. SLA-5850, Brooks Instrument, Hatfield, PA, USA) for supplying a tunable stream of air, a sample holder (flexible silicone tube assuring perfect fitting and adherence to the cylindrical sample) and an electronic differential manometer (AMECAL ST-8890, AML Instruments, Lincoln, United Kingdom) to measure the pressure drop between the inlet and the outlet of the sample.

The gas permeability through the porous samples was expressed considering Forchheimer's Eq. (1) for compressible fluids [46]:

$$(P_i^2 - P_o^2)/2\,P_oL = (\mu/k_1)\,v_s + (\rho/k_2)\,v_s^2 \quad (1)$$

where P_i is the gas pressure at the inlet and Po the one at the outlet of the sample with thickness L, measured as a function of the fluid velocity ν_s, calculated with respect to the open section of the tube.

The collected data were fitted according to the least-squares method to a parabolic model, in Eq. (2):

$$y = ax + bx^2, \quad (2)$$

where y is $(P_i^2 - P_o^2)/2\,P_oL$, and x is the fluid velocity ν_s [46].

The Darcian (k_1, m^2) and non-Darcian (k_2, m) permeabilities were then calculated from the model constants a and b as $k_1 = \mu/a$ and $k_2 = \rho/b$, considering gas viscosity (1.84 10^{-5} Pa s) and density (1.185 kg/m^3) at room temperature.

Compressive strength of selected composite foams was assessed using a Zwick-Roell Z050 universal testing machine (Ulm, Germany) with a crosshead speed of 2 mm/min.

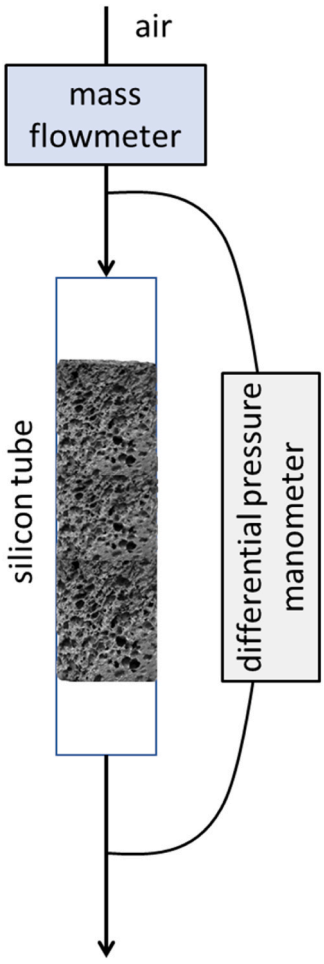

Fig. 1. Laboratory plant for permeability tests.

2.3. Preliminary gasification tests

To assess the effectiveness of the developed foams to act as catalysts for tar removal, the most promising formulation based on results of the materials characterization was chosen and tested in a lab-scale AISI316 reactor. The lab-scale plant (Fig. 2) consisted of two interconnected 22 mm ID, 500 mm length tubes installed in a Carbolite 1200 electric furnace operated at a pre-set temperature of 900 °C. In the first reactor, an olive pomace biomass was gasified by feeding it in batches of 1.0 g (totaling 5.0 g) through a sealed chamber into the top end of the reactor, on the bottom of which 7 cm of alumina wool were placed to sustain the fuel sample. In the second reactor a base layer of insulating alumina wool was arranged as in the previous case, then 3 monolithic foams were placed on top of each other to achieve the desired height in the column. The catalysts were then plugged with a second layer and laterally covered with a mica tape, to avoid lateral passages of gas and prevent any bypass. Downstream the catalytic reactor, an 80 mm filter made of alumina wool at room temperature was placed to collect the tar formed during the biomass gasification and quantify the effectiveness of the catalyst. The wool traps were weighted before the test and after water removal in desiccator the weight difference corresponding to the tar residue; the tar yield was obtained as the ratio to the weight of used biomass and the tar decomposition capacity as the relative percent ratio calculated by comparing with non-catalytic test, following the same procedure adopted before for granular geopolymer based catalyst [28].

After the gasification test, the foams were collected from the reactor and characterized in their macro and microstructure by optical and electronic microscopy, mercury intrusion porosimetry (MIP) and X-Ray

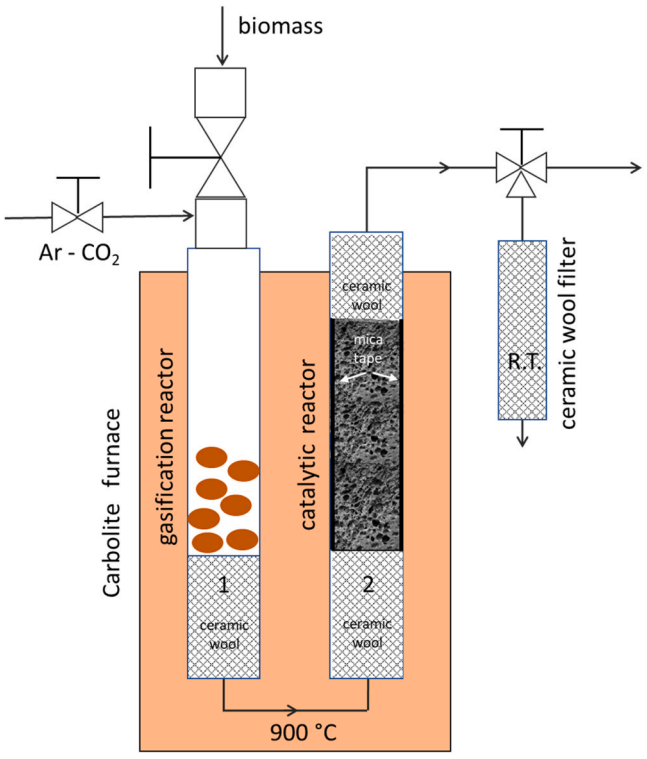

Fig. 2. The lab-scale plant for preliminary gasification tests.

diffractometry, in order to evaluate the stability and behavior of the material during the gasification cycling at 900 °C.

3. Results and discussion

3.1. Macro and microstructural analysis

The images of the samples after thermal treatment at 900 °C highlighted the different macrostructure generated via the two distinct polymer templates (Figs. 3 and 4). Cellulose-derived foams were easy-to-handle, while polyurethane-based ones proved to be fragile and delicate already in handling.

P-derived foams exhibited a neat cellular structure, with regular open cavities sized from about 1.5–3 mm (Fig. 4a). The struts delimiting the cells and shaping the entire P-derived foam structure had a thickness of approximately 0.3 mm, but they were affected by numerous local cracks (Fig. 4a). These defects, in addition to the internal cavity (Fig. 4a inset) generated during the burn out, make the structure too fragile to be reliable in a working environment. For this reason, P-derived foams were discarded for subsequent characterizations, as not properly suitable for being used in a reactor.

The cellulose-derived foams (Fig. 4b,c) had an irregular structure showing lamellar struts and macropores of one order of magnitude smaller than P-derived foams. Thanks to their hydrophilic nature, cellulose sponges were intimately permeated by the aqueous geopolymer slurry, yielding open cells with compact wall structure after thermal treatment. For this reason, although some microcracks were detected on the cellulose-based scaffolding, they did not prove to be such as to compromise the final resistance of the material.

Furthermore, the cellulose sponge, acted as a positive template for the foam at multiscale level, generating an interconnected network of multidimensional pores (Fig. 4b, c; Fig. 5). Further, a second-order inner fine porosity was detected in the strut material, deriving from intrinsic mesopores in geopolymer binder [34]. In fact, the effect of the heat treatment at 900 °C was coalescence which affected the micro-mesopore network [28], probably generating more favorable conditions for the passage of the gas flow. Furthermore, newly formed vitreous phases were observed which locally smoothed the surface texture (Fig. 5). The persistence of partially vitrified phases in the materials can be functional to an increased efficacy of the catalysts in working conditions, as the presence of unstable phases likely promoted the subsequent formation of mixed metal oxides and silicates, with higher catalytic activity [28,44].

3.2. Porosity characterization

The geometric density values and porosity characteristics obtained for the cellulose-derived foams are reported in Table 2. Fig. 6 reports the corresponding pore size distribution and cumulative pore volume obtained by MIP for GFe-C and GMnFe-C.

Both samples highlighted a quasi bi-modal porosity distribution (Fig. 6), with pore sizes mainly concentrated in a first range of 0.2–0.4 μm, and 10–18 μm or 5–10 μm for GFe-C and GMnFe-C respectively. Consistently, pore surface area from MIP analysis resulted in higher values for sample GMnFe-C, owing to its higher total open porosity and smaller average pore diameter.

To assess the porosity undetected by MIP, i.e pores sizing more than 100 μm, the image analysis was performed on cross sections of the foams. Fig. 7 showed an almost identical distribution of ultramacropores between the two samples GFe-C and GMnFe-C, confirming, as expected, how the different metal oxides play no significant role in defining the macrostructural properties of the material, which remain defined mostly by the cellulosic template. The distribution of the Feret diameter for the two materials, in fact, follows the same trend for both samples, with a frequency peak found for the size range of 0.1–0.3 mm, respectively around 45% and 49% for GFe-C and GMnFe-C, and decreasing frequencies for larger diameters, up to a maximum of 4.8 mm for GFe-C and 3.1 mm for GMnFe-C.

Pore size and pore volume MIP analysis highlighted a higher total open porosity for sample GMnFe-C, which derives from higher fractions, compared to GFe-C, of very small pores (<0.1 μm), as well as of those about 10 μm in size, contributing to the cumulative pore volume.

The images of Fig. 7 suggest a higher contribution of pores larger than 100 μm to the total porosity for GFe-C than GMnFe-C foams, as it could be expected based on their differences in total porosity and MIP open porosity (Table 2). However, the contribution of closed pores should be considered, as is the case for the voids possibly formed by an imperfect impregnation of the cellulose template, which is more likely in the case of more viscous slurry, as GFe, owing to the finer particle size of

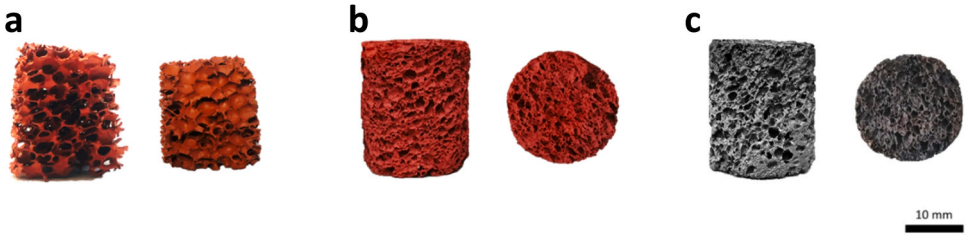

Fig. 3. Foams GFe-P (a), GFe-C (b), and GMnFe-C (c).

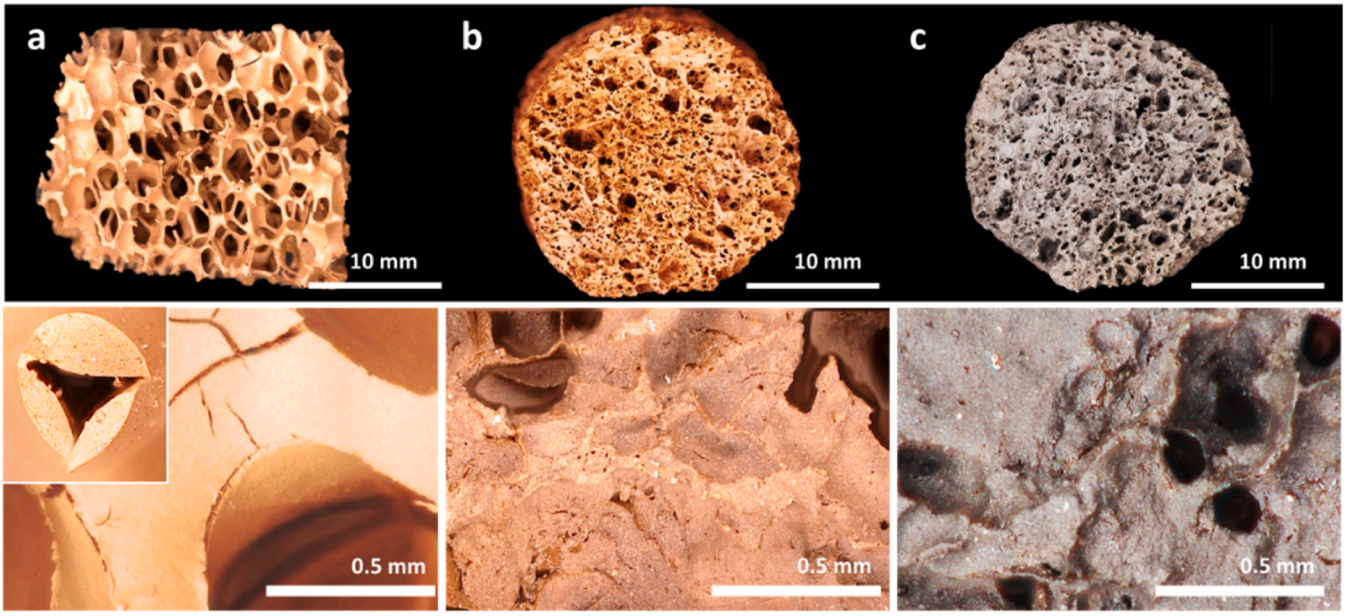

Fig. 4. Digital optical microscopy of GFe-P (a), GFe-C (b) and GMnFe-C (c) foams.

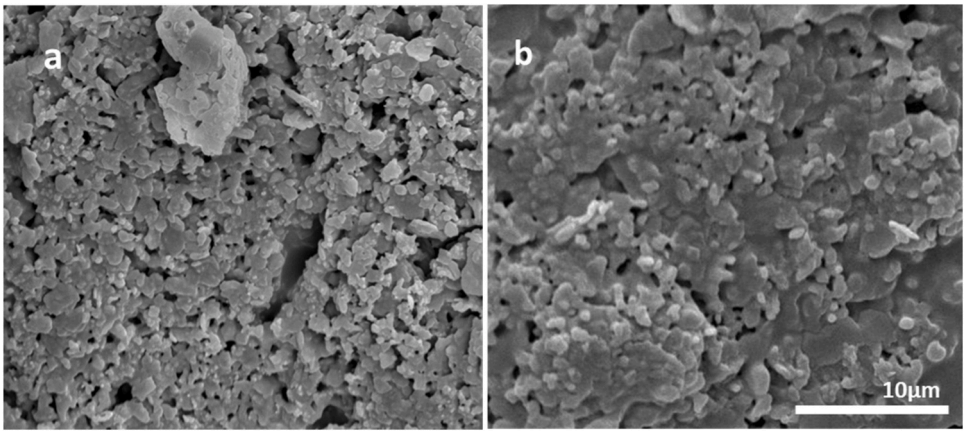

Fig. 5. SEM images for GFe-C (a) and GMnFe-C (b).

Table 2
Porosity characteristics of the foams (*from MIP).

Code	Geometric Density (g/cm^3)	Total Porosity (%)	Pore volume* (mm^3/g)	Total Open Porosity* (%)	Average pore diameter* (µm)	Median pore diameter* (µm)	Modal pore diameter* (µm)	Pore surface area* (m^2/g)
GFe-C	0.30 ± 0.01	87	363	52	0.23	0.38	0.35	6.33
GMnFe-C	0.41 ± 0.01	82	525	75	0.14	0.47	0.38	14.7

Fe_2O_3 powder compared to Mn_2O_3. Thus, the impregnation process resulted more effective in the case of geopolymer added with mixed Mn and Fe oxides than with the finer Fe oxide alone.

3.3. Phase composition

Fig. 8 shows the phase composition of GFe-C and GMnFe-C samples. As evident from the reported spectra, both samples appeared highly crystalline where the main identified phases, namely iron oxide Fe_2O_3 and manganese oxide Mn_2O_3, are consistent with the initial composition of the materials. Traces of quartz and leucite were also spotted in both samples, respectively deriving from impurity of starting metakaolin and from the crystallization of the amorphous species of the geopolymer [36].

At this stage, no evidence of newly formed mixed phases, as mixed metal silicates, could be evidenced in the samples, confirming the initial stability of the formulations after the thermal treatment and crystallization at 900 °C.

Since previous study [28] has demonstrated a better catalytic performance for geopolymer added with mixed Mn and Fe oxides than Fe oxide alone, GMnFe-C foam was selected for further functional characterizations, i.e. permeability, compressive strength and catalytic test.